Chem. Senses 36: 791–797, 2011

doi:10.1093/chemse/bjr054
Advance Access publication June 16, 2011

The Cellular Prion Protein Is Expressed in Olfactory Sensory Neurons of Adult Mice but Does Not Affect the Early Events of the Olfactory Transduction Pathway

Michele Dibattista[1,3], Maria Lina Massimino[2], Devendra Kumar Maurya[1], Anna Menini[1], Alessandro Bertoli[2] and M. Catia Sorgato[2]

[1]SISSA, International School for Advanced Studies and Italian Institute of Technology, SISSA Unit, Via Bonomea 265, 34136 Trieste, Italy and [2]Department of Biological Chemistry, University of Padova and C.N.R. Institute of Neuroscience, Viale G. Colombo 3, 35131 Padova, Italy

Correspondence to be sent to: Anna Menini, SISSA, International School for Advanced Studies and Italian Institute of Technology, SISSA Unit, Via Bonomea 265, 34136 Trieste, Italy. e-mail: menini@sissa.it

[3]Present address: Monell Chemical Senses Center, 3500 Market Street, Philadelphia, PA 19104, USA

Accepted May 20, 2010

Abstract

A conformational conversion of the cellular prion protein (PrP^C) is now recognized as the causal event of fatal neurodegenerative disorders, known as prion diseases. In spite of long-lasting efforts, however, the physiological role of PrP^C remains unclear. It has been reported that PrP^C is expressed in various areas of the olfactory system, including the olfactory epithelium, but its precise localization in olfactory sensory neurons (OSNs) is still debated. Here, using immunohistochemistry tools, we have reinvestigated the expression and localization of PrP^C in the olfactory epithelium of adult congenic mice expressing different PrP^C amounts, that is, wild-type, PrP-knockout, and transgenic PrP^C-overexpressing animals. We found that PrP^C was expressed in OSNs, in which, however, it was unevenly distributed, being detectable at low levels in cell bodies, dendrites and apical layer, and more abundantly in axons. We also studied the involvement of PrP^C in the response of the olfactory epithelium to odorants, by comparing the electro-olfactograms of the 3 mouse lines subjected to different stimulation protocols. We found no significant difference between the 3 PrP genotypes, supporting previous reports that exclude a direct action of PrP^C in the early signal transduction activity of the olfactory epithelium.

Key words: electro-olfactogram, olfaction, olfactory epithelium, PrP^C

Introduction

Up to now, the worldwide reputation of the cellular prion protein (PrP^C) has been mainly restricted to its capacity to generate prions, the infectious agents responsible for fatal neurodegenerative disorders—known as prion diseases—that include Creutzfeldt–Jakob disease (CJD) in humans, scrapie in sheep, and the so-called mad cow disease. It is now acknowledged that the disease originates when PrP^C undergoes a conformational conversion into an aberrant isoform (PrP^{Sc}), which is the major component of prions, and which is able to self-propagate into host organisms and to cause neuronal demise (Prusiner 1982, 1998; Aguzzi et al. 2008).

Noteworthy, the conservation among the vertebrate subphylum of PrP^C, which is tethered to the plasma membrane via a glycolipid anchor, has long been taken to indicate that the protein serves important functions in almost all tissues, from development throughout the entire lifespan (Linden et al. 2008). However, despite the extensive research of the past 2 decades, the precise function of PrP^C has not yet been fully elucidated. Research has also exploited murine lines in which the gene coding for PrP^C was ablated (PrP-KO) by different gene-targeting strategies (Büeler et al. 1992; Manson et al. 1994; Mallucci et al. 2002). These animals, however, displayed only marginal, if any, phenotypes under normal conditions (Criado et al. 2005; Nazor et al. 2007). Identification of the physiological role of PrP^C thus remains a major challenge not only for understanding PrP^C biology under healthy conditions but also for developing suitable means to prevent and cure prion diseases.

The search for PrP^C function has also considered the olfactory system, following the observation that PrP^C is expressed in both the olfactory epithelium and olfactory bulb (Salès et al. 1998, 2002; Moya et al. 2000; Liu et al. 2001; Ford et al. 2002; Le Pichon and Firestein 2008; Atoji and Ishiguro 2009). Interestingly, the pathologic PrP^{Sc} form of the prion protein was found to accumulate in the olfactory epithelium of individuals affected by sporadic CJD (Zanusso et al. 2003, 2009). This observation could imply that olfactory sensory neurons (OSNs) express PrP^C in sufficiently high amounts to support prion replication, and dissemination of infectivity through nasal fluids, as recently proposed (Bessen et al. 2010). Yet, it is not clear whether, in addition to axons, PrP^C localizes also in the cell body and dendrite of OSNs (Ford et al. 2002; Le Pichon and Firestein 2008).

The first step in the perception of odorants occurs in the olfactory epithelium of the nasal cavity that harbors OSNs. OSNs are bipolar neurons with a single dendrite that terminates in a knob from where several cilia protrude. Odorant molecules bind to odorant receptors in the cilia, initiating the olfactory transduction cascade that evokes a so-called generator potential in OSNs (Breer 2003; Pifferi, et al. 2009). Through a single axon, OSNs propagate the electrical signal to second-order neurons in the olfactory bulb that, in turn, project to the olfactory cortex and from here to other brain areas (Menini et al. 2004; Tirindelli et al. 2009).

A recent study has suggested a possible functional role for PrP^C in olfaction (Le Pichon et al. 2009). This conclusion stemmed from the observation that the absence of PrP^C led to the impairment of 2 types of odorant-mediated behaviors—the cookie finding and the olfactory habituation/dishabituation—whereby PrP-KO mice resulted significantly slower in finding buried food and had altered behaviors in the detection and discrimination of different odorants, respectively. Importantly, both phenotypes were rescued by transgenic neuronal-specific expression of PrP^C. The study has also demonstrated that the olfactory epithelium of PrP-KO mice had normal odorant-evoked electro-olfactogram (EOG), in contrast to substantial electrophysiologic alterations displayed by the olfactory bulb. Also in this case, the phenotype disappeared in a mouse line in which PrP^C expression was absent from only the olfactory epithelium. These findings thus allowed concluding that the olfactory deficits probably arose from an impaired processing at the level of the olfactory bulb, and/or higher "centers," rather than from modifications in the periphery. Although undoubtedly supporting a role of PrP^C in the odorant processing of the olfactory bulb, this study did not investigate whether PrP^C governed important aspects of the odorant-evoked EOG at the level of the olfactory epithelium, for example, the sensitivity, kinetics, and adaptation of the response.

In the present work, we have analyzed the localization of PrP^C in the olfactory epithelium and compared the odorant-evoked functional properties of the epithelium derived from 3 murine lines expressing different PrP^C amounts. These included wild-type (WT) FVB mice, a congenic PrP-KO line, and a transgenic line overexpressing PrP^C (PrP-OE) around 4-fold the normal level. Our study has shown that PrP^C is abundant in the axons of OSNs, but that it can also be observed in the cell body, dendrite, and ciliary layer of OSNs. We also studied the amplitude, kinetics, and adaptation properties of the odorant-evoked EOG of the olfactory epithelium. Our results further substantiate that PrP^C is not involved in the early events of the olfactory transduction pathway.

Materials and methods

Animals

We used 3-month-old male WT mice with FVB genotype (Harlan) and congenic (FVB) mice genetically modified for PrP^C expression. The latter included PrP-KO mice (line F10) and transgenic PrP-OE mice (line Tg37) (Mallucci et al. 2002) (both were kindly provided by the MRC Prion Unit). For experiments, mice were anesthetized with CO_2 inhalation before decapitation. All animals were handled in accordance with the Italian (D.L. no. 116/1992) and EU (no. 86/609/EEC) laws concerning the care and use of laboratory animals.

Immunohistochemistry

Olfactory epithelium immunostaining was performed as previously described (Pifferi, Dibattista, et al. 2009) with minor modifications. Briefly, nasal sections were fixed in 4% paraformaldehyde (4 h, 4°C), decalcified by incubation in 0.5-M ethylenediaminetetraacetic acid for 2 days, and then equilibrated overnight (4°C) in 30% (w/v) sucrose for cryoprotection. Coronal sections (16-μm thick) were cut with a cryostat and stored (–20°C) until use. For antigen retrieval, sections were treated (15 min) with Na dodecyl sulfate (0.5% v/v) in phosphate-buffered saline (PBS), incubated (90 min) in a blocking solution (2% normal goat serum [v/v] and 0.2% [v/v] Triton X-100 in PBS) and then (overnight, 4°C) with the primary antibody (Ab, diluted in the blocking solution). After rinses with 0.1% (v/v) Tween 20 in PBS (PBS-T), sections were added with the fluorophore-conjugated secondary Ab (diluted in PBS-T, 2 h, Room Temperature), rinsed, treated (30 min) with 4'-6-diamidino-2-phenylindole (0.1 μg/ml) to stain nuclei, rinsed again, and mounted with Vectashield (Vector Laboratories). We used the following primary Ab (dilutions in parenthesis): anti-PrP mouse monoclonal Ab 8H4 (1:300, a kind gift of Dr M. S. Sy, Case Western University) and goat polyclonal Ab against the olfactory marker protein (OMP) (1:600, Wako Chemicals Inc.). The Alexa 488–conjugated goat anti-mouse Ab and the Alexa 594–conjugated rabbit anti-goat Ab (1:300, Molecular Probes-Invitrogen) were the used secondary Abs. The fluorescent signal was visualized with a Leica TCS SP2 confocal microscope (Leica Microsystems). Images were acquired using a Leica software (at 1024 × 1024 pixel resolution) and analyzed with the ImageJ software. Reported

images were unmodified except for balancing brightness and contrast.

EOG recordings

EOG recordings were obtained using a method similar to that reported by Zhao et al. (1998), as previously described (Franceschini et al. 2009; Pifferi, Dibattista, et al. 2009; Cygnar et al. 2010). Immediately after decapitation, the mouse head was cut sagitally to expose the medial surface of the olfactory turbinates. EOG was measured at the surface of the olfactory epithelium (Scott and Scott-Johnson 2002). Amyl acetate was the used odorant molecule that, prepared as a 5-M stock solution (in dimethyl sulfoxide [DMSO]), was diluted with water to obtain the working concentrations (in the 5×10^{-4} to 0.5-M range). Response to DMSO alone was always less than 0.05 mV. The vapor-phase odorant stimulus was generated by placing 0.9 ml of the desired amyl acetate solution in a 10-ml glass test tube capped with a rubber stopper. Two 20-gauge needles provided the input and output ports for the vapor above the solution. For stimulation, single or paired pulses (at 8 psi) of the odorant-containing vapor were injected into a continuous stream of humidified air. Pulses were generated by a Picospritzer solenoid-controlled valve (Intracel). The minimum interval between each stimulus protocol was of at least 1 min. The odorant stimulus pathway was cleaned by air between each stimulus presentation. Experiments were performed at room temperature.

EOG kinetics was analyzed on the basis of the following 3 parameters: 1) the latency of the response, calculated as the interval between the beginning of the odorant application and the time at which the response reached 1% of the maximal value; 2) the rise time, calculated as the time interval between 1% and the peak value of the response; and 3) the time constant of the exponential fit of the recovery phase of the response, calculated over the time period from the peak value to 10% of the peak.

Recording electrodes were borosilicate glass pipettes (WPI, Sarasota) pulled (with a PP-830 puller, Narishige) and fire-polished to obtain a tip of 10–20 μm diameter. Electrodes were filled with a mammalian Ringer's solution (containing 0.6% agarose and [in mM] 140 NaCl, 5 KCl, 1 $CaCl_2$, 1 $MgCl_2$, 10 HEPES [pH 7.4], 10 glucose, 1 Na pyruvate) and mounted in a pipette holder containing an Ag/AgCl wire connected to the head stage of a patch-clamp amplifier (Multiclamp 700B). The latter was controlled by the Clampex 10.2 software via a digitizer (Digidata 1400, Molecular Devices). Electrical signals were low-pass filtered at 25 Hz and digitized at a sampling rate of 1 kHz. The ground electrode was located in the mouse brain.

Statistics

Data are reported as mean ± standard error of the mean, and n is the number of used mice. Statistical significance was evaluated by ANOVA (Igor Software, Wavemetrics), with a P value <0.05 being considered significant.

Results

Expression of PrP^C in the olfactory epithelium of adult mice

To clarify the involvement of PrP^C in odorant perception, we first examined the protein localization in the different areas of the olfactory epithelium. To this end, we analyzed by confocal microscopy epithelium coronal sections fluorescently labeled with Ab to PrP^C and OMP (a marker for mature OSNs, Baker et al. 1989). Figure 1 reports such micrographs pertaining to WT (panels A–C), PrP-OE (D–F), and PrP-KO (G–I) mice. For clarity, the different areas of the olfactory epithelium are marked in panel C, whereby AL denotes the apical region containing OSN dendritic knobs and cilia; OSN, the area with cell bodies and dendrites of OSNs; and BL, the underlying basal lamina. At the bottom of each micrograph, arrows indicate one of several axon bundles that cluster beneath the basal lamina and project to the olfactory bulb. In WT mice (panel A), we observed a weak staining for PrP^C in the OSN layer, in contrast to the intense staining of the apical region containing dendritic

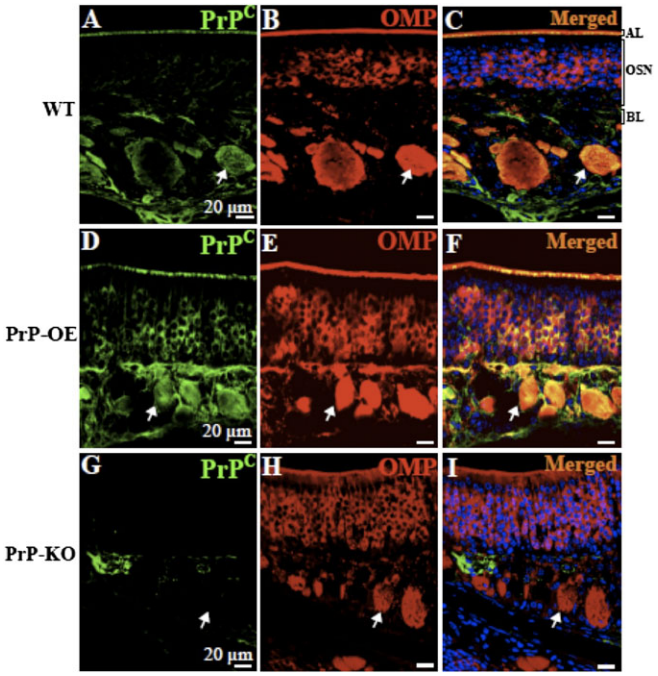

Figure 1 Expression and localization of PrP^C in the olfactory epithelium. Confocal micrographs were taken from the coronal section of the olfactory epithelium (immunostained with monoclonal Ab 8H4 to PrP^C [left panels] and a polyclonal Ab to OMP [middle panels]) obtained from adult WT **(A–C)**, PrP-OE **(D–F)**, and PrP-KO **(G–I)** mice. Some areas of the olfactory epithelium are indicated on the right of panel C: the apical layer, containing dendritic knobs and cilia (AL); the area with cell bodies and dendrites of OSNs (OSN); and the basal lamina (BL). Examples of axon bundles are indicated by white arrows. Images on the right result from the merge of left and middle images. Cell nuclei were stained by 4′-6-diamidino-2-phenylindole. Scale bar: 20 μm in all panels. This figure appears in color in the online version of *Chemical Senses*.

knobs and cilia and the even stronger signal of axon bundles (arrow). Expectedly, PrP^C localization became more clearly evident in PrP-OE mice, in particular in the OSN layer with cell bodies and dendrites (panel D). As for the PrP-KO olfactory epithelium (panel G), there was no immunoreactive signal for PrP^C, thus indicating the specificity of the used anti-PrP Ab.

Labeling of epithelia with an Ab against OMP (panels B, E, H) and the merging of this signal with that for PrP^C revealed that PrP^C and OMP colocalized in PrP^C-expressing samples (panels C and F). This is better appreciated in the magnified micrographs of the epithelium sections reported in Figure 2. Here, in spite of PrP^C faint staining (A), colocalization of PrP^C and OMP could be traced in some WT OSNs (indicated by arrows in panels A–C), which became more frequent in PrP-OE neurons (panels D–F). Interestingly, although colocalization of the 2 fluorescent signals was not evident in all PrP-OE OSNs, those in which it was present clearly indicate that the 2 proteins colocalized in the cell body, dendrite, and dendritic knob. Finally, lack of PrP^C signals in PrP-KO specimen (panels G–I) corroborates the previous conclusion on the specificity of the anti-PrP Ab.

EOG recordings in adult mice

In light of the widespread distribution of PrP^C in OSNs, we measured the EOGs of the 3 available mouse lines to understand whether PrP^C plays a role in the olfactory transduction pathway. In response to odorants, the EOG records the electrical activity of a population of OSNs as a negative electrical field potential at the surface of the epithelium, which represents the integration of generator potentials from individual OSNs (Ottoson 1955; Scott and Scott-Johnson 2002).

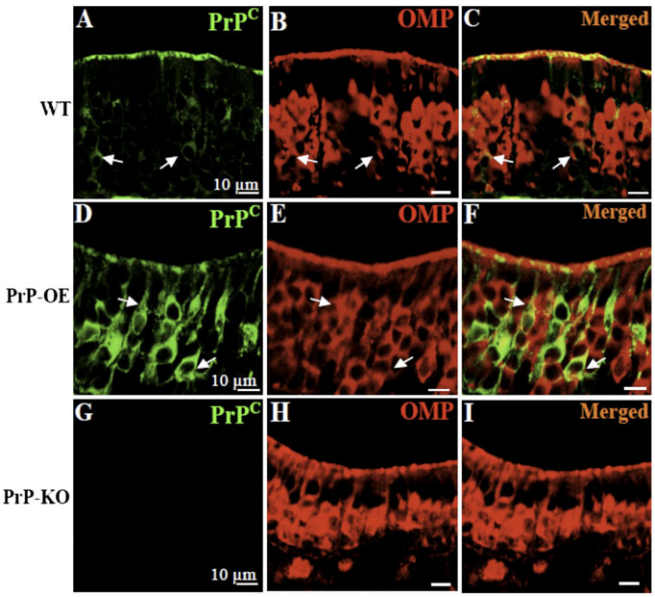

Figure 2 Magnified micrographs of PrP^C localization in OSNs. **(A–C)** The immunohistochemical staining of WT OSNs for PrP^C and OMP shows that PrP^C is present in the apical region and in the cell body of some neurons (A), while the merge of the signals for PrP^C and OMP (B) indicates that the 2 proteins colocalize, although sparsely (C). **(D–F)** Instead, the immunohistochemical staining of PrP-OE shows that the fluorescent PrP^C signal is more intense in the cell bodies and is evident also in dendrites (D, lower and upper arrow, respectively) and that the co-localization between PrP^C and OMP (F) is evident in more neurons than observed in WT samples. **(G–I)** The signal for PrP^C is absent from PrP-KO OSNs. Scale bars: 10 µm in all panels. This figure appears in color in the online version of *Chemical Senses*.

In the first set of experiments, we tested the response of the epithelium after delivery of a single 100-ms pulse of the vapor phase of a 0.5-M amyl acetate solution. Amyl acetate was the chosen odorant because it produces large responses from mouse olfactory epithelia (Zhao et al. 1998). Figure 3A reports representative EOGs of the olfactory epithelium from WT, PrP-KO, and PrP-OE mice, which were recorded at the turbinate IIb location. As shown, the response had a similar shape irrespective of the PrP genotype. Additionally, the responses also remained similar when EOGs were recorded at the turbinate III location of the epithelium (data not shown). Importantly, no significant difference was observed in the average peak amplitude of the 3 responses (Figure 3B, left panel), also when decreasing odorant concentrations were used (Figure 3B, right panel). The latter result indicates that the 3 mouse lines had equal sensitivity to odorants.

Next, we analyzed EOG kinetics, by estimating the latency and the rise time of the response, and the time constant of the termination phase at various odorant concentrations (see Materials and Methods). Once again, none of these parameters varied significantly among WT, PrP-KO, and PrP-OE epithelia (Figure 4).

It is well known that, if exposed to a prolonged odorant stimulus, or to repetitive brief stimuli, OSNs undergo an adaptive decrease of the response amplitude. To verify whether this phenomenon was dependent on PrP^C, we first recorded EOG responses elicited by a continuous (5-s pulse) odorant stimulation. As illustrated in Figure 5A, reporting representative EOGs from the olfactory epithelium of WT, PrP-KO, and PrP-OE mice exposed to 5×10^{-3} M amyl acetate, the response amplitude progressively declined with comparable kinetics irrespective of PrP^C expression levels. Further, the extent of adaptation, calculated as the percentage decrease between the peak value and the response amplitude at the end of the stimulus (Figure 5A), did not significantly change between samples, also when exposed to different odorant concentrations (Figure 5B).

We then analyzed the adaptation phenomenon induced by repetitive brief odorant stimuli, consisting in 2 identical 100-ms pulses separated by a 3-s time interval. Here, also the representative EOG responses shown in Figure 6A, which were elicited by a double pulse of 5×10^{-2} M amyl acetate, indicate that samples with different PrP genotypes exhibited comparable adaptation behaviors. No significant difference in the extent of adaptation, calculated as the ratio between the second and the first peak amplitude, was observed among WT, PrP-KO, and PrP-OE olfactory epithelia exposed to different odorant concentrations (Figure 6B).

Taken together, the above reported EOG responses, recorded in WT, PrP-KO, and PrP-OE mice after

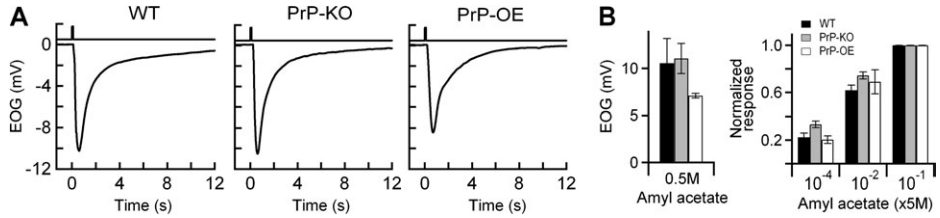

Figure 3 Amplitude and sensitivity of odorant responses at the turbinate IIb location. **(A)** Representative EOG recordings in response to 100-ms pulses (delivered at the time indicated in the top trace) of the odorant vapor from a 0.5-M amyl acetate solution. **(B)** Bar diagrams of the average peak amplitude of EOGs elicited by a pulse from the 0.5-M odorant solution (left panel) show that the response was not significantly different among olfactory epithelia from WT, PrP-KO, or PrP-OE mice (n = 4–6). Similarly, no significant difference between WT, PrP-KO, and PrP-OE mice was observed when decreasing odorant concentrations were used (right panel). In this case, for each PrP genotype, the peak values of the EOG response at each odorant concentration were normalized to those recorded at 0.5 M. Reported values are mean ± standard error of the mean (n = 4).

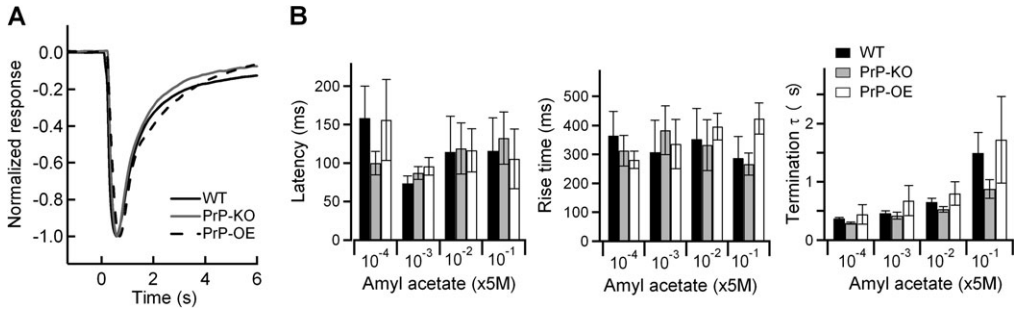

Figure 4 Kinetics parameters of the odorant response. **(A)** EOG responses to a 100-ms pulse of vapor from the 0.5-M amyl acetate solution from WT (black trace), PrP-KO (gray trace), and PrP-OE (dotted trace) epithelia were normalized to the respective peak value. Normalized traces underscore that EOG responses had comparable kinetics irrespective of the PrP genotype. **(B)** Latency (left panel), rise time (middle panel), and time constant of the termination phase (right panel) of EOG responses to different odorant concentrations. In no case, significant differences were observed between WT, PrP-KO, and PrP-OE samples. Reported values are mean ± standard error of the mean (n = 4).

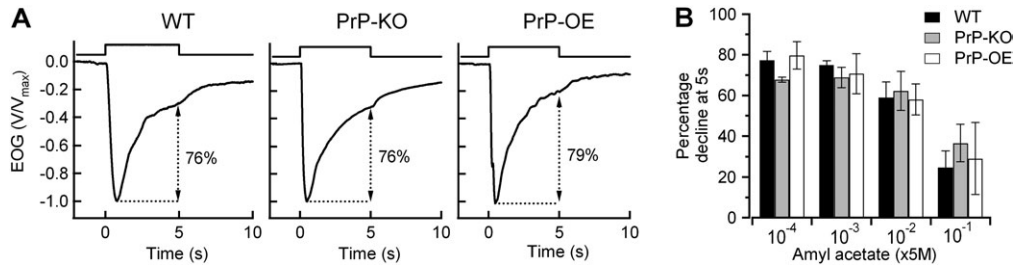

Figure 5 Adaptation to a continuous odorant stimulus. **(A)** Representative EOG responses to a 5-s pulse of 5×10^{-3} M amyl acetate by WT, PrP-KO, and PrP-OE olfactory epithelia. Each trace was normalized to the respective peak value. Top traces report the stimulation protocol. The decrease in response amplitude in the presence of the prolonged odorant stimulus, determined as the percentage reduction in amplitude between the peak and the value recorded at the end of the 5-s stimulus, did not significantly change in samples with different PrP^C levels. **(B)** No significant difference in the extent of adaptation between WT, PrP-KO, and PrP-OE mice was observed also when the continuous 5-s pulses were delivered using different odorant concentrations. Reported values are mean ± standard error of the mean (n = 4).

application of different stimulation protocols, clearly indicate that PrP^C did not significantly affect the response to odorants at the level of the olfactory epithelium.

Discussion

Although several studies have reported that axons of OSNs harbor high quantities of PrP^C (Salès et al. 1998; Moya et al. 2000; Ford et al. 2002; Le Pichon and Firestein 2008; Atoji and Ishiguro 2009), to the best of our knowledge only 2 of these reports have analyzed in detail the expression and distribution of the protein in the entire olfactory epithelium (Ford et al. 2002; Le Pichon and Firestein 2008). However, these studies did not clarify whether PrP^C expression was restricted to axons of OSNs (Le Pichon and Firestein 2008) or whether the protein was also present in neuronal cell bodies and dendrites (Ford et al. 2002). In the present study, we re-examined the issue also by taking advantage of transgenic mice with about 4-fold overexpression of PrP^C. This allowed us to better visualize PrP^C neuronal

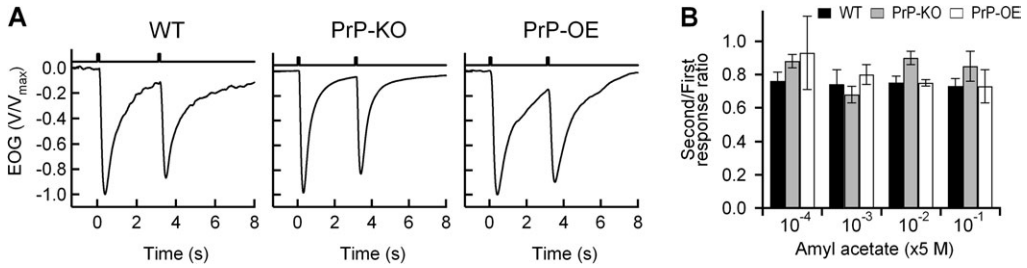

Figure 6 Adaptation to repeated odorant stimuli. **(A)** Representative EOG responses to 2 identical 100-ms pulses of 5×10^{-2} M amyl acetate, separated by a 3-s time interval. Each trace was normalized to the amplitude value of the first peak. The double pulse stimulation protocol is illustrated in the top traces. Comparable adaptive decreases in the amplitude of the second peak, with respect to the first one, were observed in samples with different PrP^C levels. **(B)** Also when different odorant concentrations were used, the extent of adaptation, evaluated as the ratio between the second and the first peak amplitude, was similar in WT, PrP-KO, and PrP-OE olfactory epithelia. Reported values are mean ± standard error of the mean (n = 4).

distribution and to demonstrate that the protein was localized in all areas of OSNs, although at uneven levels. Indeed, although PrP^C maximal expression was undoubtedly in axons, lower amounts of the protein could nevertheless be detected in cell bodies, dendrites, and in the cilia-containing apical layer.

Several reasons may explain the discrepancy between our findings and those previously reported. These include the methodology for preparing the olfactory epithelium and the specificity and sensitivity of the used anti-PrP^C antibodies. A further source of variability can be tentatively identified in the different genotypes of the mouse models under investigations (FVB mice in our study, compared with 129/Ola, Ford et al. 2002, and B6129, Le Pichon and Firestein 2008, strains used in the previous works), which may have originated subtle, yet detectable, differences in PrP^C expression and distribution.

The olfactory phenotype previously reported in PrP-KO mice (Le Pichon et al. 2009), and the broad distribution of PrP^C in OSNs reported here, prompted us to analyze in detail the possible involvement of PrP^C in the response to odorants of the olfactory epithelium of adult (FVB) mice. In this context, it is worth noting that a number of studies, carried out also with PrP-KO paradigms, have suggested that PrP^C could play a role in the control of Ca^{2+} homeostasis in neurons (Sorgato and Bertoli 2009; Lazzari et al. 2011). Hence, because Ca^{2+} plays a central role in the olfactory transduction cascade at the level of both excitation and adaptation to odorants (Menini 1999; Matthews and Reisert 2003), it was interesting to verify whether the response to odorants was altered in PrP-KO and/or PrP-OE OSNs.

However, comparison of EOG recordings, which measure the generator potentials of a population of OSNs in response to odorants (Ottoson 1955; Scott and Scott-Johnson 2002), showed no statistically significant variation in the amplitude and kinetics of the response to short odorant pulses by the olfactory epithelium of WT, PrP-KO, and PrP-OE mice. In addition, comparable extents of adaptive phenomena, induced by both prolonged odorant exposure and repetitive brief odorant pulses, were equally observed in the olfactory epithelia expressing different PrP^C levels.

In conclusion, our results definitively establish that PrP^C does not affect the EOG response of the olfactory epithelium to odorants. The EOG, however, allows estimating the capability of the olfactory epithelium to transduce the odorant stimulus into generator potentials, but not the production and transmission of action potentials. Our findings, therefore, cannot yet rule out the possibility that PrP^C plays a role in the generation of action potentials in OSNs and/or in their propagation to the axon terminals. In addition, given that olfactory nerve terminals release glutamate to stimulate second-order neurons in the olfactory bulb, another intriguing possibility could be that PrP^C influences Ca^{2+}-dependent glutamate release at the presynaptic level. This hypothesis seems reasonable also in view of the above-mentioned implication of PrP^C in regulating Ca^{2+} homeostasis. Thus, before definitively ruling out a physiological role of PrP^C in the response to odorants by the olfactory epithelium, further experiments need to address the above described hypotheses.

Funding

Italian Ministry of Education, University, and Research (Prin 2008 to M.C.S), the Italian Institute of Technology (to A.M.), and the University of Padova (Progetto d'Ateneo CPDA089551 to A.B.).

References

Aguzzi A, Sigurdson C, Heikenwaelder M. 2008. Molecular mechanisms of prion pathogenesis. Annu Rev Pathol. 3:11–40.

Atoji Y, Ishiguro N. 2009. Distribution of the cellular prion protein in the central nervous system of the chicken. J Chem Neuroanat. 38:292–301.

Baker H, Grillo M, Margolis FL. 1989. Biochemical and immunocytochemical characterization of olfactory marker protein in the rodent central nervous system. J Comp Neurol. 285:246–261.

Bessen RA, Shearin H, Martinka S, Boharski R, Lowe D, Wilham JM, Caughey B, Wiley JA. 2010. Prion shedding from olfactory neurons into nasal secretions. PLoS Pathogens. 6:e1000837.

Breer H. 2003. Sense of smell: recognition and transduction of olfactory signals. Biochem Soc Trans. 31:113–116.

Büeler H, Fischer M, Lang Y, Bluethmann H, Lipp HP, DeArmond SJ, Prusiner SB, Aguest M, Weissmann C. 1992. Normal development and behaviour of mice lacking the neuronal cell-surface PrPC protein. Nature. 356:577–582.

Criado JR, Sánchez-Alavez M, Conti B, Giacchino JL, Wills DN, Henriksen SJ, Race R, Manson JC, Chesebro B, Oldstone MB. 2005. Mice devoid of prion protein have cognitive deficits that are rescued by reconstitution of PrP in neurons. Neurobiol Dis. 19:255–265.

Cygnar K, Stephan AB, Zhao H. 2010. Analyzing responses of mouse olfactory sensory neurons using the air-phase electroolfactogram recording. J Vis Exp. 37:1850.

Ford MJ, Burton LJ, Li H, Graham CH, Frobert Y, Grassi J, Hall SM, Morris RJ. 2002. A marked disparity between the expression of prion protein and its message by neurons of the CNS. Neuroscience. 111:533–551.

Ford MJ, Burton LJ, Morris RJ, Hall SM. 2002. Selective expression of prion protein in peripheral tissues of the adult mouse. Neuroscience. 113: 177–192.

Franceschini V, Bettini S, Pifferi S, Rosellini A, Menini A, Saccardi R, Ognio E, Jeffery R, Poulsom R, Revoltella R. 2009. Human cord blood CD133+ stem cells transplanted to nod-scid mice provide conditions for regeneration of olfactory neuroepithelium after permanent damage induced by dichlobenil. Stem Cells. 27:825–835.

Lazzari C, Peggion C, Stella R, Massimino ML, Lim D, Bertoli A, Sorgato MC. 2011. Cellular prion protein is implicated in the regulation of local Ca2+ movements in cerebellar granule neurons. J Neurochem. 5:881–890.

Le Pichon CE, Firestein S. 2008. Expression and localization of the prion protein PrP(C) in the olfactory system of the mouse. J Comp Neurol. 508:487–499.

Le Pichon CE, Valley MT, Polymenidou M, Chesler AT, Sagdullaev BT, Aguzzi A, Firestein S. 2009. Olfactory behavior and physiology are disrupted in prion protein knockout mice. Nat Neurosci. 12:60–69.

Linden R, Martins VR, Prado MAM, Cammarota M, Izquierdo I, Brentani RR. 2008. Physiology of the prion protein. Physiol Rev. 88:673–728.

Liu T, Zwingman T, Li R, Pan T, Wong BS, Petersen RB, Gambetti P, Herrup K, Sy MS. 2001. Differential expression of cellular prion protein in mouse brain as detected with multiple anti-PrP monoclonal antibodies. Brain Res. 30:118–129.

Mallucci GR, Ratté S, Asante EA, Linehan J, Gowland I, Jefferys JGR, Collinge J. 2002. Post-natal knockout of prion protein alters hippocampal CA1 properties, but does not result in neurodegeneration. EMBO J. 21:202–210.

Manson JC, Clarke AR, Hooper ML, Aitchison L, McConnell I, Hope J. 1994. 129/Ola mice carrying a null mutation in PrP that abolishes mRNA production are developmentally normal. Mol Neurobiol. 8:121–127.

Matthews HR, Reisert J. 2003. Calcium the two-faced messenger of olfactory transduction and adaptation. Curr Opin Neurobiol. 13: 469–475.

Menini A. 1999. Calcium signalling and regulation in olfactory neurons. Curr Opin Neurobiol. 9:419–426.

Menini A, Lagostena L, Boccaccio A. 2004. Olfaction: from odorant molecules to the olfactory cortex. News Physiol Sci. 19:101–104.

Moya KL, Salès N, Hässig R, Créminon C, Grassi J, Di Giamberardino L. 2000. Immunolocalization of the cellular prion protein in normal brain. Microsc Res Tech. 50:58–65.

Nazor KE, Seward T, Telling GC. 2007. Motor behavioral and neuropathological deficits in mice deficient for normal prion protein expression. Biochim Biophysica Acta. 1772:645–653.

Ottoson D. 1955. Analysis of the electrical activity of the olfactory epithelium. Acta Physiol Scand Suppl. 35:1–83.

Pifferi S, Dibattista M, Sagheddu C, Boccaccio A, Al Qteishat A, Ghirardi F, Tirindelli R, Menini A. 2009. Calcium-activated chloride currents in olfactory sensory neurons from mice lacking bestrophin-2. J Physiol. 587:4265–42–79.

Pifferi S, Menini A, Kurahashi T. 2009. Signal transduction in vertebrate olfactory cilia. In: Menini A, editor. The neurobiology of olfaction. Boca Raton (FL): CRC Press, Taylor & Francis Group. p. 203–224.

Prusiner SB. 1982. Novel proteinaceous infectious particles cause scrapie. Science. 216:136–144.

Prusiner SB. 1998. Prions. Proc Natl Acad Sci U S A. 95:13363–13383.

Salès N, Hässig R, Rodolfo K, Di Giamberardino L, Traiffort E, Ruat M, Frétier P, Moya KL. 2002. Developmental expression of the cellular prion protein in elongating axons. Eur J Neurosci. 15:1163–1177.

Salès N, Rodolfo K, Hässig R, Faucheux B, Di Giamberardino L, Moya KL. 1998. Cellular prion protein localization in rodent and primate brain. Eur J Neurosci. 10:2464–2471.

Scott JW, Scott-Johnson PE. 2002. The electroolfactogram: a review of its history and uses. Microsc Res Tech. 58:152–160.

Sorgato MC, Bertoli A. 2009. From cell protection to death: may Ca2+ signals explain the chameleonic attributes of the mammalian prion protein? Biochem Biophys Res Commun. 379:171–174.

Tirindelli R, Dibattista M, Pifferi S, Menini A. 2009. From pheromones to behavior. Physiol Rev. 89:921–956.

Zanusso G, Ferrari S, Benedetti D, Sbriccoli M, Rizzuto N, Monaco S. 2009. Different prion conformers target the olfactory pathway in sporadic Creutzfeldt-Jakob disease. Ann N Y Acad Sci. 1170:637–643.

Zanusso G, Ferrari S, Cardone F, Zampieri P, Gelati M, Fiorini M, Farinazzo A, Gardiman M, Cavallaro T, Bentivoglio M, et al. 2003. Detection of pathologic prion protein in the olfactory epithelium in sporadic Creutzfeldt-Jakob disease. N Engl J Med. 348:711–719.

Zhao H, Ivic L, Otaki JM, Hashimoto M, Mikoshiba K, Firestein S. 1998. Functional expression of a mammalian odorant receptor. Science. 279:237–242.